

# Modelling the Geometry of Geological Units and its Uncertainty in 3D From Structural Data: The Potential-Field Method

J P Chilès<sup>1</sup>, C Aug<sup>1</sup>, A Guillen<sup>2</sup> and T Lees<sup>3</sup>

## ABSTRACT

Most 3D geological modelling tools were designed for the needs of the oil industry and are not suited to the variety of situations encountered in other application domains. Moreover, the usual modelling tools are not able to quantify the uncertainty of the geometric models generated. The potential-field method was designed to build 3D geological models from data available in geology and mineral exploration, namely the geological map and a DTM, structural data, borehole data and interpretations of the geologist. This method considers a geological interface as a particular isosurface of a scalar field defined in the 3D space, called a potential field. The interpolation of that field, based on universal cokriging, provides surfaces that honour all the data.

Due to the difficulty of inferring the covariance of the potential field, the first implementation of the method used an *a priori* covariance given by the user. New developments allow this covariance to be identified from the structural data. This makes it possible to associate sensible cokriging standard deviations to the potential-field estimates and to express the uncertainty of the geometric model.

Practical implementation issues for producing 3D geological models are presented: how to handle faults, how to honour borehole ends, how to take relationships between several interfaces into account, how to integrate gravimetric and magnetic data.

An application to the geological modelling of the Broken Hill district, Australia, is briefly presented.

## INTRODUCTION

The resource evaluation of a mining deposit is often decomposed in two steps:

1. delimitation of the boundaries of the units corresponding to the various geological formations or ore types; and
2. estimation of grades within each unit.

In simple cases (eg a series of subhorizontal layers), the geometric model can be built using 2D geostatistical techniques (kriging or cokriging of the elevations or thicknesses of the various horizons), which also quantify the uncertainty of the model. A lot of effort has been undertaken to develop 3D modelling tools capable of handling more complex situations (eg Mallet, 2003). Most of them were designed to fulfil the needs of the oil industry, namely for situations where a draft of the underground model can be defined from seismic data. Deterministic methods are also available to interpolate between subparallel interpreted cross-sections.

When assessing resources, the knowledge of the degree of uncertainty of the estimation is as important as the estimate itself. The uncertainty on the boundaries and volumes of the various units is often a major part of the global uncertainty. When 2D geostatistical techniques can be used, the quantification of that uncertainty by an estimation variance is a valuable by-product of the estimation process. By contrast usual 3D modelling tools are not able to quantify the uncertainty attached to the interpolated model, whereas that uncertainty can be quite large.

The potential-field method was designed to build 3D geological models from data available in geology and mining exploration, namely:

1. a geological map and a digital terrain model (DTM),
2. structural data related to the geological interfaces,
3. borehole data, and
4. interpretations from the geologist.

It is not limited to sedimentary deposits and does not require seismic data (such data would be useful but is seldom available in geological, mining and civil engineering applications). It can be linked to inverse methods to take gravimetric and/or magnetic data into account.

The potential-field method defines a geological interface as an implicit surface, namely a particular isosurface of a scalar field defined in the 3D space – the potential field. The 3D interpolation of that potential field, based on universal cokriging, provides isosurfaces that honour all the data. Since no data measures the potential field itself, its covariance cannot be inferred directly, so that the method was used with a covariance chosen by the user, thus making the method a conventional one, among others. Recent developments allow that covariance to be determined from the structural data, which makes it possible to associate sensible cokriging standard deviations to potential-field estimates and to translate them into uncertainties on the 3D model.

We will first recall the basic principle of the method, present the inference of the potential-field covariance from the structural data and explain how the uncertainty of the 3D model can be quantified. We will then examine several practical issues: how to handle faults, how to honour borehole ends, how to take relationships between several interfaces into account, how to link 3D geometrical modelling and inverse modelling of gravimetric and magnetic data. We will end with a brief presentation of an application to the geological modelling of the Broken Hill district, Australia, and a short discussion.

## BASIC PRINCIPLE OF THE POTENTIAL-FIELD METHOD

The basic method – which will be generalised in the sequel – is designed to model a geological interface or a series of subparallel interfaces  $I_k$ ,  $k = 1, 2, \dots$  (Lajaunie, Courrioux and Manuel, 1997). Its principle is to summarise the geology by a potential field, namely a scalar function  $T(\mathbf{x})$  of any point  $\mathbf{x} = (x, y, z)$  in 3D space, designed so that the interface  $I_k$  corresponds to an isopotential surface, ie the set of points  $\mathbf{x}$  that satisfies  $T(\mathbf{x}) = t_k$  for some unknown value  $t_k$  of the potential field. Equivalently, the geological formation encompassed between two successive interfaces  $I_k$  and  $I_{k+1}$  is defined by all the points  $\mathbf{x}$  whose potential-field value lies in the interval defined by  $t_k$  and  $t_{k+1}$ . In figurative terms, in the case of sedimentary deposits,  $T$  could be seen as the time of deposition of the grain located at  $\mathbf{x}$ , or at least as a monotonous function of that geological time, and an interface as an isochron surface. This figurative interpretation can be adequate in some applications but is not necessary for the development of the method.

1. Centre de Géostatistique, École des Mines de Paris, 35 rue Saint-Honoré, 77305 Fontainebleau cedex, France.

2. Bureau de Recherches Géologiques et Minières (BRGM), BP 6009, 45060 Orléans cedex 2, France.

3. School of Geosciences, Monash University, Victoria.

**Data types**

$T(\mathbf{x})$  is modelled with two kinds of data, as shown in Figure 1:

1. points known to belong to the interfaces  $I_1, I_2, \dots$ , typically 3D points discretising geological contours on the geological map and intersections of boreholes with these interfaces; and
2. structural data: in the case of sedimentary rocks whose stratification is parallel to the geological horizons, this data is polarised unit vectors normal to the stratification; similarly they can be unit vectors orthogonal to foliation planes for metamorphic rocks; this data is measured on outcrops or in boreholes, either on the interfaces or anywhere within a formation.

For the interpolation of the potential field, this data is coded as follows:

1. Since the potential value at  $m + 1$  points  $\mathbf{x}_0, \mathbf{x}_1, \dots, \mathbf{x}_m$  sampled on the same interface is not known, this data is taken as  $m$  increments  $T(\mathbf{x}_\alpha) - T(\mathbf{x}'_\alpha)$ ,  $\alpha = 1, \dots, m$ , all valued to 0. Two classical choices for  $\mathbf{x}'_\alpha$  consist in taking either the point  $\mathbf{x}_0$  whatever  $\alpha$ , or the point  $\mathbf{x}_{\alpha-1}$  (the choice has no impact on the result; other choices are possible provided that the increments are linearly independent). Since the sampled data can be located on several interfaces, let  $M$  represent the total number of increments (it is equal to the total number of data points on the interfaces, minus the number of interfaces).
2. The polarised unit vector normal to each structural plane is considered as the gradient of the potential field, or equivalently as a set of three partial derivatives  $\partial T(\mathbf{x}) / \partial u, \partial T(\mathbf{x}) / \partial v, \partial T(\mathbf{x}) / \partial w$  at some point  $\mathbf{x}_\beta$ . The coordinates  $u, v, w$  are defined in an orthonormal system; this system can be the same for all the points or a specific system can be attached to each point (the result does not depend on the

choice provided that the three partial derivatives are taken in consideration). In the sequel let  $\partial T(\mathbf{x}_\beta) / \partial u_\beta$  denote any partial derivative at  $\mathbf{x}_\beta$  and  $N$  denote the total number of such data (in practice  $N$  is a multiple of three and the  $\mathbf{x}_\beta$  form triplets of common points). Let us recall that the  $\mathbf{x}_\beta$  do not necessarily coincide with the  $\mathbf{x}_\alpha$  (the latter are located on the interfaces whereas the former can be located anywhere).

**Interpolation of the potential field**

The potential field is then only known by discrete or infinitesimal increments. It is thus defined up to an arbitrary constant. So an arbitrary origin  $\mathbf{x}_0$  is fixed and at any point  $\mathbf{x}$  the potential increment  $T(\mathbf{x}) - T(\mathbf{x}_0)$  is kriged. The estimator is in fact a cokriging of the form:

$$T^*(\mathbf{x}) - T^*(\mathbf{x}_0) = \sum_{\alpha=1}^M \mu_\alpha (T(\mathbf{x}_\alpha) - T(\mathbf{x}'_\alpha)) + \sum_{\beta=1}^N v_\beta \frac{\partial T}{\partial u_\beta}(\mathbf{x}_\beta)$$

where the weights  $\mu_\alpha$  and  $v_\beta$ , solution of the cokriging system, are in fact functions of  $\mathbf{x}$  (and  $\mathbf{x}_0$ ). One may wonder why the potential increments are introduced in that estimator since their contribution is nil. Because, and this is key, the weights  $v_\beta$  are different from weights based on the gradient data alone. Conversely, the gradient data also play a key role, because in their absence the estimator would be zero whatever  $\mathbf{x}$  may be.

Cokriging is performed in the framework of a random function model.  $T(\cdot)$  is assumed to be a random function with a polynomial drift:

$$m(\mathbf{x}) = \sum_{\ell=0}^L b_\ell f^\ell(\mathbf{x})$$

and a stationary covariance  $K(\mathbf{h})$ . Since the vertical usually plays a special role, the degree of the polynomial drift can be higher vertically than horizontally and the covariance can be anisotropic. For example, if we model several subparallel and subhorizontal interfaces, it makes sense to assume a vertical linear drift of the form  $m(\mathbf{x}) = b_0 + b_1 z$ , ie with two basic drift functions  $f^0(\mathbf{x}) \equiv 1$  and  $f^1(\mathbf{x}) = z$ . A geological body with the shape of an ellipsoid would correspond to a quadratic drift, ie to the ten basic monomial drift functions with degree less than or equal to two. Note, however, that the drift function  $f^0(\mathbf{x}) \equiv 1$  shall be forgotten in any case since the potential increments as well as the partial derivatives filter  $b_0$ . In theory, sinusoidal terms could be added too (Dimitrakopoulos and Luo, 1997), but in usual applications geology is not regular enough for that.

Once the basic functions  $f^\ell(\mathbf{x})$  of the drift and the covariance  $K(\mathbf{h})$  of  $T(\cdot)$  are known, we have all the ingredients to perform a cokriging in the presence of gradient data, as shown in Chilès and Delfiner (1999, section 5.5.2). Indeed, the drift of  $\partial T(\mathbf{x}) / \partial u$  is simply  $\partial m(\mathbf{x}) / \partial u$ , ie a linear combination of the partial derivatives  $\partial f^\ell(\mathbf{x}) / \partial u$  with the same unknown coefficients  $b_\ell$  as for  $m(\mathbf{x})$ , the covariances of partial derivatives are second-order partial derivatives of  $K(\cdot)$ , and the cross-covariances of the potential field and partial derivatives are partial derivatives of  $K(\cdot)$ .

**Implementation of the cokriging algorithm**

Since the potential increment data in fact do not contribute to the final cokriging estimate, the estimator can be seen as an integration of the gradient data. To preserve the spatial continuity of the cokriging estimates it is wise to work in unique neighbourhood, namely to effectively include all the data in the cokriging of  $T(\mathbf{x})$ , whatever  $\mathbf{x}$  may be. If we are not interested in the cokriging variance, cokriging can be implemented in its dual form, which has two advantages:

1. the cokriging system is solved once for all, which saves computing time; and

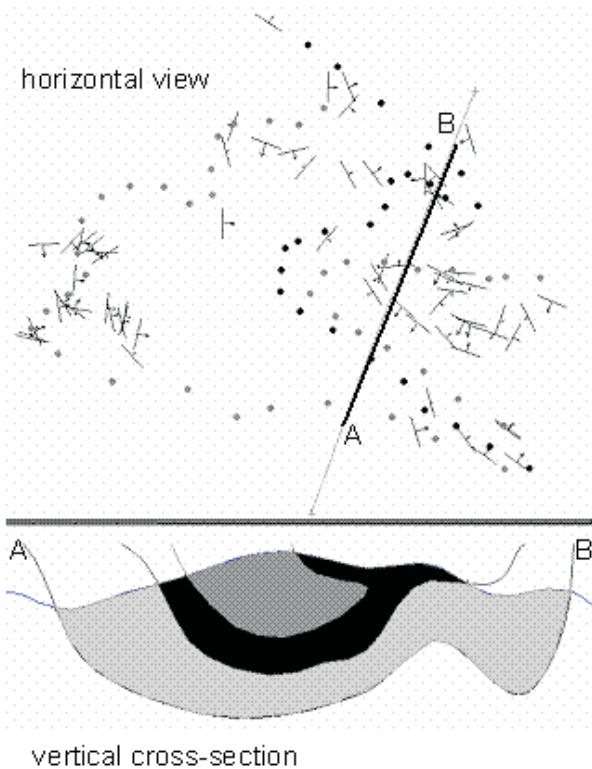


FIG 1 - Principle of the potential-field method. Top: surface data – points at interfaces and structural data; bottom: vertical cross-section through the 3D model (Courrioux *et al*, 1998).

- that form is especially suited when cokriging is considered as an interpolator, because it allows an easy estimation of  $T(\mathbf{x}) - T(\mathbf{x}_0)$  at any new point  $\mathbf{x}$ .

The latter property is very useful to display 3D views of the geological model with an algorithm such as the marching cube, which starts from the estimation of  $T(\mathbf{x}) - T(\mathbf{x}_0)$  at the nodes of a coarse regular grid and then requires intermediate points to be predicted to track the desired isopotential surface.

### INFERENCE OF THE COVARIANCE OF THE POTENTIAL FIELD

In usual geostatistical applications, the covariance or variogram of the variable under study is modelled from the sample variogram of the data. In the present case, we have no measurement of the potential  $T(\mathbf{x})$ , and the potential increments used for the interpolation cannot be used for the inference of  $K$  since they all have a zero value. In its first implementation, the algorithm was used heuristically with a covariance model arbitrarily chosen by the user. That choice had been more or less rationalised according to the following considerations:

- At the scale considered, geological interfaces are smooth rather than fractal surfaces, which implies that the covariance is twice differentiable. A cubic model was considered as a good compromise among the various possible models, because it just has the necessary regularity at the origin and has a scale parameter that can accommodate various situations.
- The scale parameter  $a$  and sill  $C$  of the covariance  $K(\mathbf{h})$  determine the sill of the variogram of the partial derivatives: it is equal to  $14 C / a^2$  in the case of an isotropic cubic covariance considered here. When there is no drift and the geological body is isotropic (eg a granitic intrusion), the unit gradient vector can have any direction so that its variance is equal to one. The variance of each partial derivative is then equal to one third. A consistent choice for  $C$  once the scale parameter  $a$  has been chosen is thus  $C = a^2 / 42$ . That value shall be considered as an upper bound for  $C$  when the potential field has a drift, because in that case the mean of the potential gradient is not equal to zero so that its variance is shorter than one (its quadratic mean is zero by definition).
- Sensible measurement variances can also be defined (nugget effects).

The use of a heuristic model, however, implies two limitations:

- the choice is usually not the best one; and
- more importantly, this precludes any evaluation of the magnitude of the interpolation error. A means to infer the covariance is thus a core issue of that approach.

Since  $K$  cannot be inferred from the potential increments, its inference shall be done with the gradient data. This is possible because the covariances of the partial derivatives derive from that of the potential field. In the case of an isotropic covariance  $K(\mathbf{h})$ , which for simplicity will be denoted  $K(r)$  as a function of  $r = \|\mathbf{h}\|$ , the covariance of, say,  $\partial T(\mathbf{x}) / \partial u$  and  $\partial T(\mathbf{x}+\mathbf{h}) / \partial u$  is  $-K''(\|\mathbf{h}\|)$  when  $\mathbf{h}$  is parallel to the  $u$  axis,  $-K'(\|\mathbf{h}\|) / \|\mathbf{h}\|$  when  $\mathbf{h}$  is orthogonal to the  $u$  axis.

The assumption of an isotropic covariance model is of course too restrictive and shall be relaxed. In practice the covariance  $K(\mathbf{h})$  is supposed to be the sum of several cubic components  $K_p(\mathbf{h})$ , each one possibly displaying a zonal or geometric anisotropy. To avoid a too great complexity, the main anisotropy axes  $u, v, w$ , are supposed to be common to all the components. More general formulae than the above ones are available for that model.

Thanks to these formulae the covariance parameters of  $K$  (nugget effect, scale parameter of each covariance component in the three main directions, sill of each component) are chosen so as to lead to a satisfactory global fit of the directional sample variograms of the three components of the gradient. An automatic fitting procedure based on the Levenberg-Marquardt method has been developed to facilitate that task (Aug, 2004).

Figure 2 shows an example of such a fitting. 1485 structural data was sampled in an area of about  $70 \times 70 \text{ km}^2$  in the Limousin (Massif Central, France). The main  $(u, v, w)$  coordinates here coincide with the geographical  $(x, y, z)$  coordinates. Since the structural data is all located on the topographic surface, the variograms have been computed in the horizontal plane only. Note that the sill of the variogram of the vertical component is much lower than that of the horizontal components. This is due to the fact that the layers are subhorizontal so that the vertical component of the gradient displays limited variations around its non-zero mean. The model  $K$  includes three components, the second of which only depends on the horizontal component of  $\mathbf{h}$  and the third one on the N-S component (zonal anisotropies).

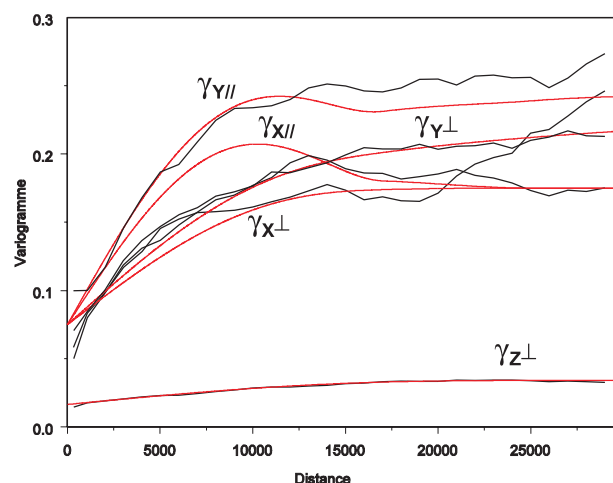


FIG 2 - Example of fitting of the covariance of the potential field from the sample variograms of the partial derivatives of the potential field. Limousin dataset, Massif Central, France.  $\gamma_{X//}$  and  $\gamma_{X\perp}$  denote the variogram of the partial derivative  $\partial T / \partial x$  respectively along and orthogonal to direction  $x$  (Aug, 2004).

### UNCERTAINTY OF THE 3D MODEL

Case studies have shown that the use of a sound covariance model improves the model in comparison with the use of a conventional model. An additional interest of using a covariance fitted from the data is the possibility to obtain sensible cokriging standard deviations. Indeed, when the covariance model is *a priori* chosen by the user, cokriging is a conventional interpolator, among others, which cannot claim for optimality, and the cokriging variance is a mere configuration index.

When the 'true' covariance of the potential field is known, a meaningful cokriging standard deviation  $\sigma_{CK}(\mathbf{x})$  can be associated with the cokriging of  $T(\mathbf{x}) - T(\mathbf{x}_0)$ . The calculation of that standard deviation requires the use of the standard form of the cokriging system, which calls for more computing time than its dual form (this is the price to pay for knowing the uncertainty attached to the geological model). Let us suppose that some geological formation is defined by the set of points  $\mathbf{x}$  such that  $T(\mathbf{x}) - T(\mathbf{x}_0)$  is comprised between two values  $t$  and  $t'$ . Under the assumption that the potential field is a Gaussian random function

– an assumption that seems reasonable in the present context – the probability that a given point  $\mathbf{x}$  belongs to that formation is:

$$\Pr\{t \leq T(\mathbf{x}) - T(\mathbf{x}_0) < t'\} = G\left(\frac{t' - (T^*(\mathbf{x}) - T^*(\mathbf{x}_0))}{\sigma_{CK}(\mathbf{x})}\right) - G\left(\frac{t - (T^*(\mathbf{x}) - T^*(\mathbf{x}_0))}{\sigma_{CK}(\mathbf{x})}\right)$$

where:

$G$  is the standard normal cumulative distribution function

Similarly, if we are interested in the interface passing by the point  $\mathbf{x}_0$ , namely in the set of points  $\mathbf{x}$  such that  $T(\mathbf{x}) - T(\mathbf{x}_0) = 0$ , the variable  $R(\mathbf{x}) = [T^*(\mathbf{x}) - T^*(\mathbf{x}_0)] / \sigma_{CK}$  measures the likelihood that  $\mathbf{x}$  belongs to the interface. Indeed, writing the obvious relation:

$$T(\mathbf{x}) - T(\mathbf{x}_0) = T^*(\mathbf{x}) - T^*(\mathbf{x}_0) + \text{cokriging error}$$

we see that  $\mathbf{x}$  belongs to the interface if and only if  $T^*(\mathbf{x}) - T^*(\mathbf{x}_0)$  is equal to minus the cokriging error, or equivalently if  $R(\mathbf{x})$  is equal to minus the standardised cokriging error (the ratio of the error by  $\sigma_{CK}(\mathbf{x})$ ). The value of that error is not known but it is a variable with zero mean and unit variance.

For example, assuming again that the potential field is Gaussian, the area defined by  $|R(\mathbf{x})| < 2$  includes about 95 per cent of the actual interface. Figure 3 displays  $R(\mathbf{x})$  for the top of the lower gneiss unit in the Limousin. The black line corresponds to  $R(\mathbf{x}) = 0$ , ie to the isovalue surface of the cokriged potential field passing by the data points sampled on that interface. The true interface is likely to be found in the light-coloured area, whereas the darkest area can be considered as a forbidden area.

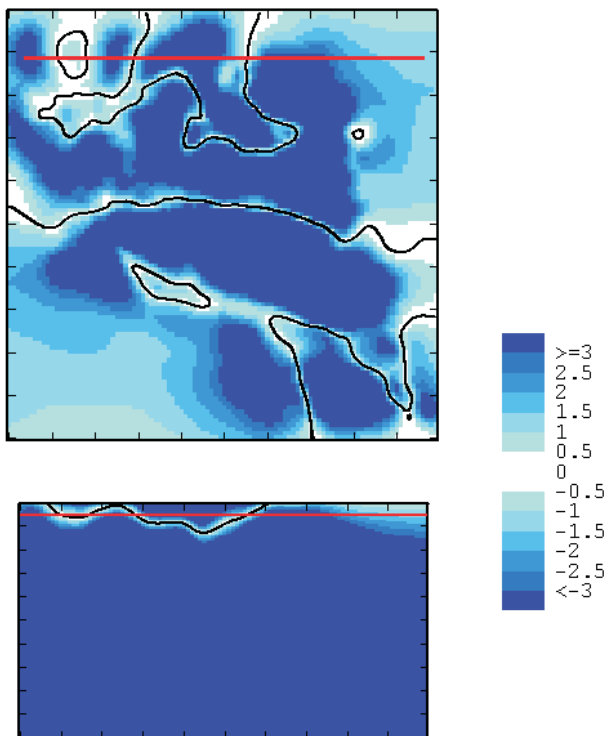


FIG 3 - Representation of the uncertainty of the top of a geological unit by the variable  $R(\mathbf{x})$  (upper gneiss unit, Limousin). The data (geological map and structural data) are all located on the topography. Top: map of a zone of 65 km  $\times$  65 km in the horizontal plane with elevation 500 m; bottom: vertical E-W cross-section with 62 km extension and 34 km depth. The black curve represents the kriged interface. The true interface is in fact in the shaded zones, with a smaller probability as the zone is darker. The darkest zones can be considered as exclusion zones (Aug, 2004).

## PRACTICAL IMPLEMENTATION ISSUES

The potential-field method has been implemented in 3D Geological Editor, software developed by BRGM (the French geological survey). In order to model real-world situations a number of practical implementation issues had to be solved.

### Modelling several interfaces

In practical applications several interfaces shall be modelled, and all of them are not subparallel. Several potential fields are then used. A stratigraphic column is defined by the geologist to determine how to combine the various potential fields. That column defines the chronological order of the interfaces as well as their nature, coded as either ‘erode’ or ‘onlap’. An ‘erode’ potential field is used for example to mask the eroded part of the previous formations or to model an intrusive body.

### Faults

Several methods can be envisaged to handle faults. If they delimit blocks and the potential field is not correlated from one block to the other, it obviously suffices to process each block separately. Another conventional technique is to consider faults as screens. This technique cannot be used in unique neighbourhood. The method used in 3D Geological Editor is thus different. It is a transposition to 3D potential fields of the method proposed by Maréchal (1984) to handle faults in the 2D interpolation of the elevation of interfaces, where faults are entered as external drift functions. This method requires the knowledge of the fault planes and also of the zones of influence of the faults.

Let us start with a very simple example, a normal fault intersecting the whole study zone and dividing it in two subzones  $D$  and  $D'$ . That fault induces a discontinuity of the potential field, whose amplitude is not known. Cokriging can accommodate that discontinuity whatever its amplitude by introducing a drift function complementing the  $L$  polynomial drift functions, for example:

$$f^{L+1}(\mathbf{x}) = 1_D(\mathbf{x}),$$

or equivalently, in a symmetrised form:

$$f^{L+1}(\mathbf{x}) = 1_D(\mathbf{x}) - 1_{D'}(\mathbf{x}).$$

If the polynomial drift functions include the monomial  $f^1(\mathbf{x}) = x$  (first coordinate) due to the presence of a linear trend of the potential field, and we have good reasons to suspect not only a discontinuity but also a change of slope of the drift when crossing the fault, it is advisable to also introduce an additional drift function such as:

$$f^{L+2}(\mathbf{x}) = x 1_D(\mathbf{x}).$$

A finite fault can be modelled with a drift function with a bounded support, and whose value vanishes on the support boundaries; inside that support, the function takes on positive values on one side of the fault plane, with a maximum at the centre of the fault, and negative values on the other side. Figure 4 illustrates in 2D how that method takes faults into account.

In real-world applications a fault plane is not exactly a planar surface. It is often only known by some points on its surface and unit vectors orthogonal to it. Its geometry can thus be modelled by a potential field too.

### Borehole ends

When processing borehole data, only the intersections of the boreholes with the interfaces are usually entered as data, whereas the borehole also carries the information that all the points between two successive interfaces belong to the same horizon.



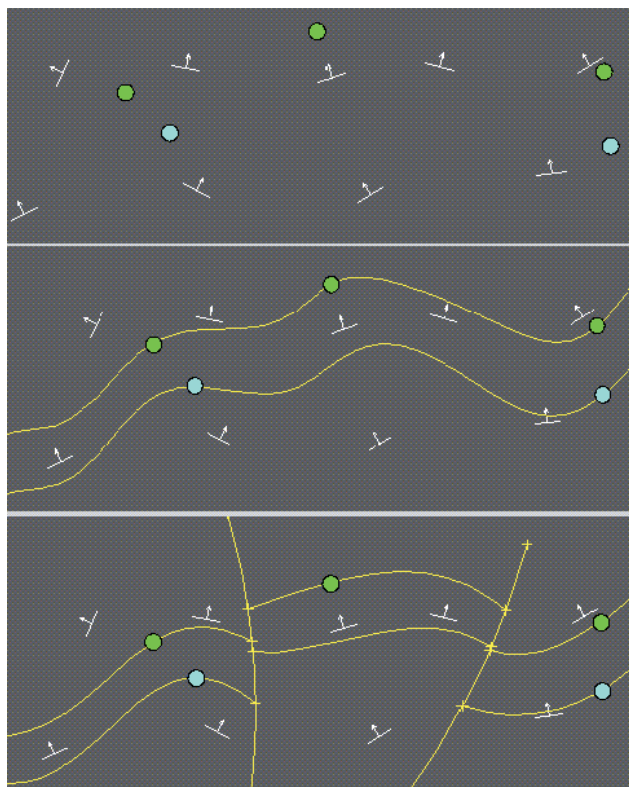


FIG 4 - Handling faults. Top: data points located on two interfaces and structural data; middle: model built without introducing any fault; bottom: model taking faults into account.

That additional information is usually redundant, so it can be legitimately disregarded. A noticeable exception is the end of a borehole: it does not coincide with an interface and gives the information that the next interface is deeper than the borehole. It is important to take that information into account, because otherwise the model can place the interface at a lower depth than the borehole. If that interface is modelled by a 2D interpolation of its elevation, such information is simply an inequality about the elevation value at the  $(x, y)$  location of the borehole. In the case of a 3D modelling of a potential field, it can also be expressed as an inequality about a potential-field increment.

Such inequalities can be taken into account by first replacing the inequality data with hard data and then applying the standard cokriging method. The critical step is of course the first one. The hard value replacing an inequality datum must be consistent with the inequality and all the other data (the hard data and the other inequality data) and with the spatial variability of the potential field. The method is rigorous when the inequality is replaced by the mathematical expectation of the potential increment conditional on all the hard and inequality data (Freulon and de Fouquet, 1993; Chilès and Delfiner, 1999). This is done with an iterative method, which is a direct application of the Gibbs sampler. Note that contrary to the usual potential field data, this new increment data is not equal to zero.

The practical implementation of the iterative process is based on a simple kriging algorithm. It is rigorous if the potential field is a Gaussian random function with known mean, because in that case kriging coincides with the conditional expectation. A Gaussian assumption does not look unnatural in our applications, but the potential fields considered usually include an unknown global drift. Aug (2004) has shown that the algorithm remains robust in the applications we consider when simple kriging is replaced by an ordinary or universal cokriging of our data. Figure 5 illustrates the consequences of using or not using that algorithm.

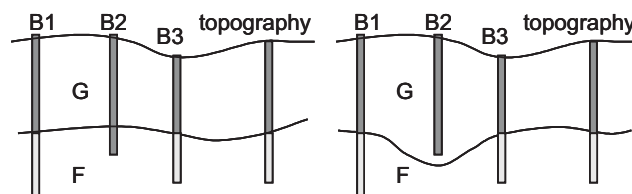


FIG 5 - Handling borehole ends. Left: end of borehole B2 not taken into account; right: end of borehole B2 taken into account.

### Coupling with an inverse modelling of geophysical data

In geological and mining exploration applications, seismic profiles as well as gravity and magnetic data are often available. Interpreted seismic cross-sections directly provide data that can be processed by 3D Geological Editor. This is not the case for gravity and magnetic data. Presently, the geological model provided by the use of the potential-field method is considered as the initial state of a constrained inverse modelling of this data.

That inversion is based on an iterative method presented by Guillen *et al* (2004), which is applied to a discrete version of the domain under study. The domain is subdivided in cubic cells, with a geological formation and a physical property (density or magnetic susceptibility) attached to each cell. At the initial state the formation derives from the potential-field model, and the value of the physical property, eg density, is randomly chosen in an *a priori* distribution for that formation. The gravity response of the model at the location of the gravity data is computed. A cell is then randomly chosen and a tentative new state is proposed by changing the formation and/or density of that cell (a formation change is proposed only if it does not alter the topology of the model); that tentative state is accepted as a new state according to whether or not it improves the response of the model in comparison with the gravity data. That procedure is iterated millions of times. In fact the decision of accepting or not accepting a proposed state is taken according to a Metropolis-Hastings dynamic, which accepts some deterioration of the gravity response of the model, especially in the early iterations, to avoid a convergence of the algorithm to a local optimum.

### APPLICATION TO THE BROKEN HILL DISTRICT

3D Geological Editor has been mainly used for geological modelling at a regional scale, especially in the Alps and the Massif Central. We present here the results of an application to geological data from the Broken Hill district, Australia.

#### Geological context

The project area is a 20 km  $\times$  20 km area (Figure 6) extending to a depth of 5 km. The rock units and their relationships, listed in Table 1, are based on the GSNSW synthesis (Willis, 1989); it is noted, however, that there is the possibility of major structures within the stratigraphy (Noble, 2000; Gibson and Nutman, 2004).

Two geological questions concerning the geometry of these units were posed at the beginning of this study:

1. Do the major units flatten at depth?
2. What is the relative importance of the different units and are they regionally extensive?

The objective was therefore to use the geological modelling tool to evaluate various geological hypotheses.

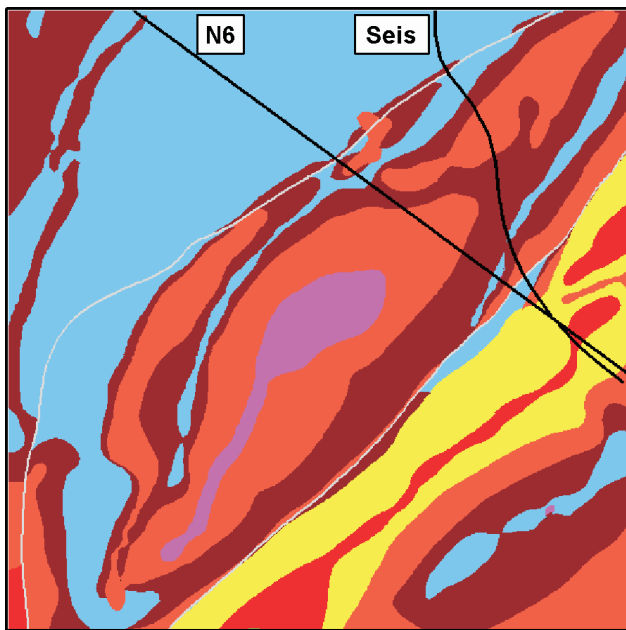


FIG 6 - Plan view of the Broken Hill geological model. The shades correspond to the geological units shown in Table 1. The presence of a fault is indicated by a white line. The location of Section N6 (Figure 7) and the seismic line are shown as black lines. The project covers an area 20 km x 20 km, with the coordinates for the top-left corner being 535000E 647000N (GDA94, MGA54).

TABLE 1  
Geological units, relationships.

Map symbol	Geological unit	Relationship
	Alma Gneiss	Intrusive (erosional)
	Paragon Group	Unconformable (onlap)
	Sundown Group	Unconformable (onlap)
	Broken Hill Group	Unconformable (onlap)
	Thackaringa Group	Unconformable (onlap)
	Thorndale Gneiss	Unconformable (onlap)
	Clevedale Migmatite	Unconformable (onlap)
	Rift Series	Unconformable (onlap)

3D Geological Editor allows the rapid construction and editing of 3D geological models that are based on input observations, supplemented by various hypothetical observations. The 3D volumetric model proposed by Pasminco (Archibald *et al*, 2000) was used as a starting point.

**Lithology**

The published geological map (Willis, 1989) was a primary input along with five regional-scale geological cross-sections. A seismic section was also used as a backdrop for digitising ‘observations’ for the Rift unit (Gibson *et al*, 1998). The final 3D model is shown as a geological map in Figure 6, and on Section N6 in Figure 7 and Section N7 in Figure 8.

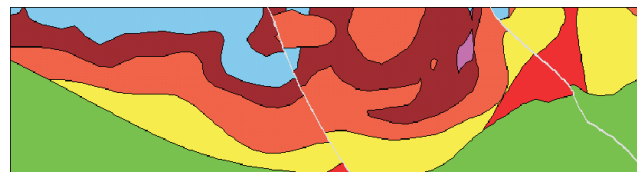


FIG 7 - Section N6 through the 3D model. (Length: 20 km; Depth: 5 km; V/H=1). The shades of the units are as shown in Table 1.

The Alma Gneiss is an intrusive body. Note that it is presented to 3D Geological Editor as being at the top of the sequence, with an erosional relationship, to be properly represented.

**Structure**

Management of faults is a key issue in constructing a realistic 3D geological model. The number of faults introduced into the model was minimised. It was found that a satisfactory geological model at this broad scale could be constructed with just two faults. Other more extensive and detailed models with up to ten faults are in preparation. Complex structural effects of the Broken Hill terrain that are represented in the model include ‘retrograde’ shears, high temperature shears, boudinage and transposition.

The 3D geological model encompasses a parallelepiped 20 km long, 20 km wide and 5 km deep (Figure 9). More details are given by Guillen *et al* (2004), along with a constrained gravity inversion where that model is considered as the *a priori* geological model.

**DISCUSSION**

The potential-field method has now reached a development level that enables it to model real-world situations, even in complex cases. For example, Maxelon (2004), and Maxelon and Mancktelow (in press), used it to model foliation fields and a juxtaposition of nappes with a strong folding in the Lepontine Alps. Some issues deserve a mention, as follows.

Rather than a cokriging we can be interested in conditional simulations. The method can be straightforwardly generalised to conditional simulations if we assume that the potential fields are Gaussian, which is not a strong assumption in this kind of application.

The covariance fitting has some part of uncertainty. To take it into account, a Bayesian approach has been developed by Aug (2004). It consists in defining an *a priori* distribution for the joint distribution of the covariance parameters and defining the corresponding distribution from the data. That posterior distribution can be incorporated in the cokriging or conditional simulation process.

A better integration of the geometric modelling and the geophysical inversion would be welcome. This could be done by starting from a conditional simulation of the geometric model and defining the state changes with regard to the uncertainty of that geometric model, to the spatial structure of the potential field, and to the spatial structure of the physical variables.

Last but not least, the gradient of a random function is only by chance a unit vector. Considering the vectors defined by the structural data as unit vectors is thus somewhat abusive. The ideal would be to sample both a structural direction and a structural intensity, but this is possible only in very specific cases. Aug (2004) has shown on simulations of actual situations that replacing actual gradients by unit vectors usually has a minor impact on the determination of the covariance and the cokriging. It could be useful, however, to improve the inference method, which could be done at least with the use of simulations.

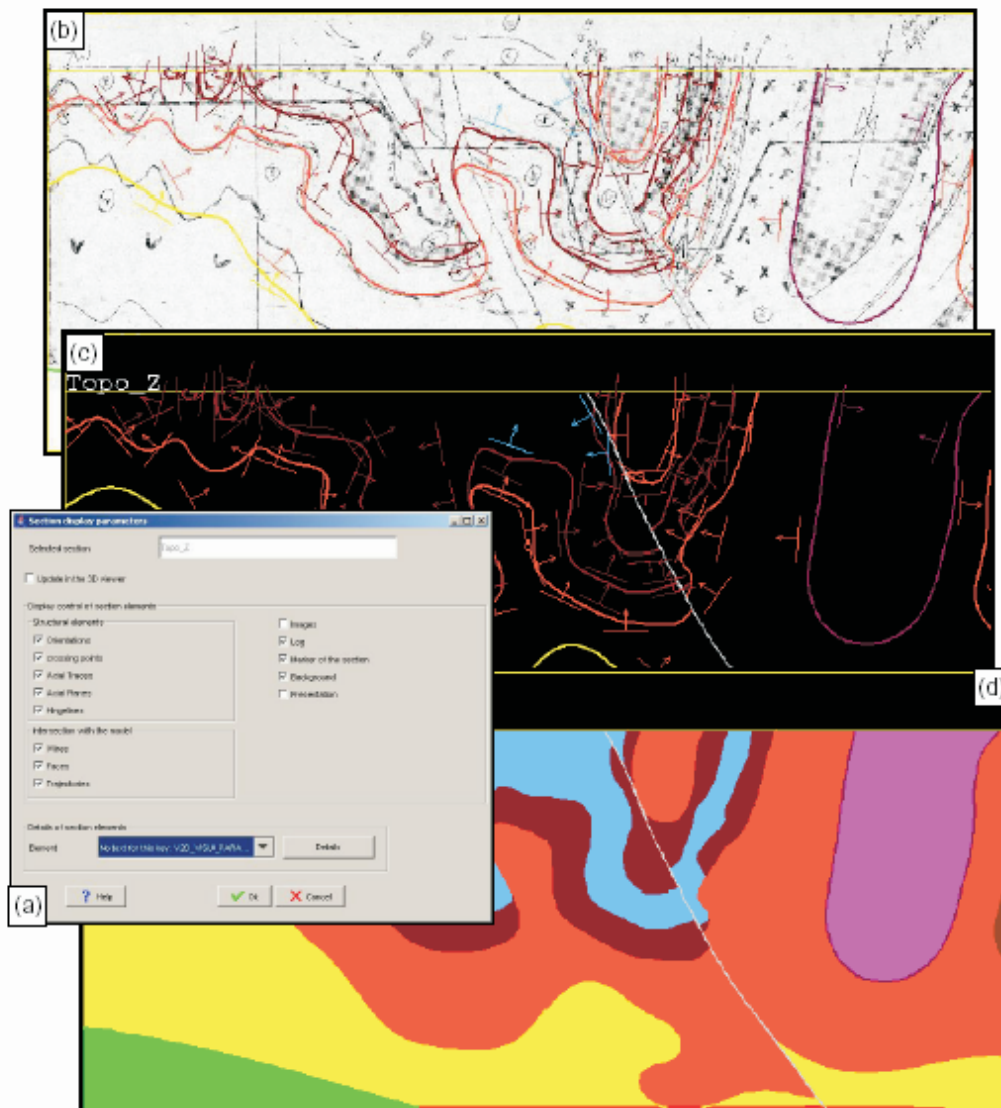


FIG 8 - Part of the geological cross-section N7. Various 'layers' can be presented in 3D Geological Editor's map and section presentations, and each of these can be turned 'on', or 'off' (a). Image (b) shows the model geology rendered as lines onto the geologist's original working section. Image (c) shows the model geology as lines, together with the orientation data. Image (d) shows the model geology as solid-geology. The user can control the plotting resolution, to achieve either fast plots, or high-resolution images, such as this one. Section length: 12.7 km, V/H=1.

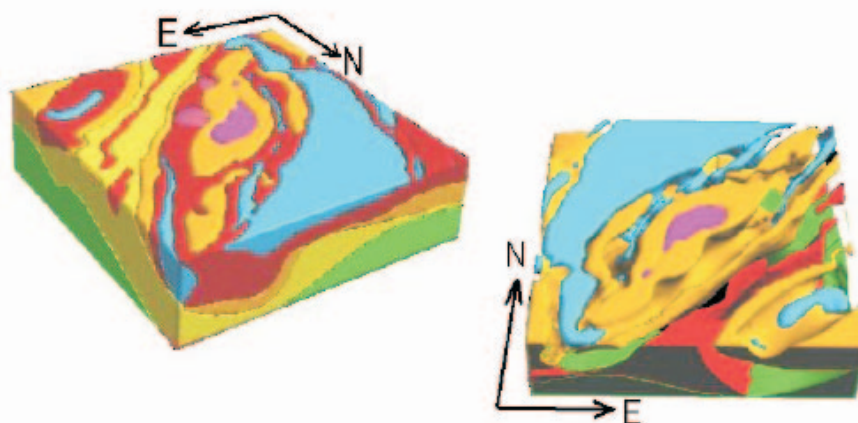


FIG 9 - Perspective view of the 3D geological model, viewed from the northeast and south west. The shades of the units are as shown in Table 1.

## ACKNOWLEDGEMENTS

The research work carried out at the École des Mines de Paris was funded by BRGM. The Broken Hill geological modelling work was undertaken by Intrepid Geophysics and was funded by an *Innovation Access Programme* grant under the Australian Government's innovation statement.

## REFERENCES

- Archibald, N J, Holden, D, Mason, R and Green, T, 2000. A 3D geological model of the Broken Hill 'line of lode' and regional area, Unpublished report, Pasminco Exploration.
- Aug, C, 2004. Modélisation géologique 3D et caractérisation des incertitudes par la méthode du champ de potentiel, PhD thesis to be defended in December 2004, École des Mines de Paris.
- Chilès, J P and Delfiner, P, 1999. *Geostatistics: Modeling Spatial Uncertainty*, 695 p (Wiley: New York).
- Courrioux, G, Lajaunie, C, Chilès, J P and Lazarre, J, 1998. Foliation fields and 3D geological modelling, in *Proceedings 3D Modeling of Natural Objects, A Challenge for 2000's*, ENS de Géologie, Nancy, Vol 1.
- Dimitrakopoulos, R and Luo, X, 1997. Joint space-time modelling in the presence of trends, in *Geostatistics Wollongong '96* (Eds: E Y Baafi and N A Schofield), Vol 1, pp 138-149 (Kluwer: Dordrecht).
- Freulon, X and de Fouquet, C, 1993. Conditioning a Gaussian model with inequalities, in *Proceedings Geostatistics Tróia '92* (Ed: A Soares), Vol 1, pp 201-212 (Kluwer: Dordrecht).
- Gibson, G, Drummond, B, Fomin, T, Owen, A, Maidment, D, Gibson, D, Peljo, M and Wake-Dyster, K, 1998. Re-evaluation of crustal structure of the Broken Hill inlier through structural mapping and seismic profiling, AGSO Record 1998/11.
- Gibson, G M and Nutman, A P, 2004. Detachment faulting and bimodal magmatism in the Palaeoproterozoic Willyama Supergroup, south-central Australia: keys to recognition of a multiply deformed Precambrian metamorphic core complex, *J Geol Soc (London)*, 161:55-66.
- Guillen, A, Courrioux, G, Calcagno, P, Lane, R, Lees, T and McInerney, P, 2004. Constrained gravity inversion applied to Broken Hill, in Extended abstracts, *ASEG 17th Geophysical Conference and Exhibition, Integrated Exploration in a Changing World*, Sydney, August.
- Lajaunie, C, Courrioux, G and Manuel, L, 1997. Foliation fields and 3D cartography in geology: principles of a method based on potential interpolation, *Mathematical Geology*, 29(4):571-584.
- Mallet, J L, 2003. *Geomodeling*, 599 p (Oxford: Oxford).
- Maréchal, A, 1984. Kriging seismic data in presence of faults, in *Geostatistics for Natural Resources Characterization* (Eds: G Verly, M David, A G Journel and A Maréchal), Part 1, pp 271-294 (Reidel: Dordrecht).
- Maxelon, M, 2004. Developing a three-dimensional structural model of the lower Lepontine Nappes – Central Alps, Switzerland and Northern Italy, PhD thesis (unpublished), ETH Zurich.
- Maxelon, M and Mancktelow, N S, in press. Three dimensional nappe geometry and tectonostratigraphy of the Pennine Zone, Central Alps, Switzerland and Northern Italy, *Earth Science Reviews*.
- Noble, M P, 2000. The geology of the Broken Hill synform, NSW, Australia, MSc thesis (unpublished), Monash University, Victoria.
- Willis, I L, 1989. *Broken Hill Stratigraphic Map* (New South Wales Geological Survey: Sydney).